Tumor-Suppressive Effects of Pannexin 1 in C6 Glioma Cells

Charles P.K. Lai,[1] John F. Bechberger,[1] Roger J. Thompson,[2] Brian A. MacVicar,[2] Roberto Bruzzone,[3] and Christian C. Naus[1]

Departments of [1]Cellular and Physiological Sciences and [2]Psychiatry, The University of British Columbia, Vancouver, British Columbia, Canada and [3]Department of Neuroscience, Institut Pasteur, Paris, France

Abstract

Mammalian gap junction proteins, connexins, have long been implicated in tumor suppression. Recently, a novel family of proteins named pannexins has been identified as the mammalian counterpart of the invertebrate gap junction proteins, innexins. To date, pannexin 1 (Panx1) and pannexin 2 (Panx2) mRNAs are reported to be expressed in the brain. Most neoplastic cells, including rat C6 gliomas, exhibit reduced connexin expression, aberrant gap junctional inter-cellular communication (GJIC), and an increased prolif-eration rate. When gap junctions are up-regulated by transfecting C6 cells with *connexin43*, GJIC is restored and the proliferation is reduced. In this study, we examined the tumor-suppressive effects of Panx1 expression in C6 cells. Reverse transcription-PCR analysis revealed that C6 cells do not express any of the pannexin transcripts, whereas its nontumorigenic counterpart, rat primary astrocytes, exhibited mRNAs for all three pannexins. On generation of stable C6 transfectants with tagged Panx1 [myc or enhanced green fluorescent protein (EGFP)], a localization of Panx1 expression to the Golgi apparatus and plasma membrane was observed. In addition, Panx1 transfectants exhibited a flattened morphology, which differs greatly from the spindle-shaped control cells (EGFP only). Moreover, Panx1 expression increased gap junctional coupling as shown by the passage of sulforhodamine 101. Finally, we showed that stable expression of Panx1 in C6 cells significantly reduced cell proliferation in monolayers, cell motility, anchorage-independent growth, and *in vivo* tumor growth in athymic nude mice. Altogether, we conclude that the loss of pannexin expression may participate in the development of C6 gliomas, whereas restoration of Panx1 plays a tumor-suppressive role. [Cancer Res 2007;67(4):1545–54]

Introduction

Connexins have been considered to be the sole mammalian gap junctional constituent proteins since their identification. More recently, sequences with low similarity to the invertebrate innexins have been identified in chordates, leading to the emergence of a novel family of proteins, called pannexins, which are also capable of forming functional hemichannels and intercellular channels (1, 2). To date, three pannexin members have been identified in vertebrates: pannexin 1 (Panx1), pannexin 2 (Panx2), and pannexin 3

(Panx3; ref. 3), and several invertebrate innexins are also referred to as pannexins (4). Although protein expression of these pannexins has not been defined in mammals due to the lack of specific antibodies, Northern blot analysis and *in situ* hybridization experiments have identified location-specific pannexin mRNA expression in rats: Panx1 is ubiquitously expressed, Panx2 is particularly abundant in the brain, and Panx3 is present in the skin (1, 5). Previous studies on innexin mutants in *Drosophila* have shown innexin-specific functions, including synaptogenesis in the giant fiber system, epithelial organization and morphogenesis, and germ cell differentiation processes (6). Although it remains to be seen whether pannexins can be regarded as vestigial innexins that have survived in higher animals, this implies that, other than connexins, pannexins may also play functional roles in chordates (6, 7).

Gap junctions are proteineous membrane channels that are located between the lateral surfaces of two adjacent mammalian cells, directly connecting their cytosols. A connexin-based gap junction is composed of two connexons, each composed of a hexamer of connexins. Each connexin has four-membrane–spanning domains, two extracellular loops, a cytoplasmic loop, and cytoplasmic NH_2 and COOH termini (8). These channels allow the direct passage of small ions and molecules with a molecular weight <1,200 Da, such as Ca^{2+} ion and cyclic AMP, and function in maintaining intercellular communication and homeostasis within and between tissues (9, 10). In accordance, gap junctions have been found to be down-regulated in many types of cancer, including gliomas, breast carcinoma, and prostate cancers (10, 11). Moreover, transfection of cDNAs encoding connexins to restore gap junctional intercellular communication (GJIC) in cancer cell models reverts some of the transformed phenotype and reduces proliferation of the neoplasms (12, 13). This suggests that connexins function as tumor suppressors and numerous studies have explored restoration of GJIC as a potential therapy against cancer (14).

Despite sequence dissimilarity between connexins and pannexins, the two protein families share predicted structural resemblance (15). Analogous to connexins, formation of pannexin-based hemichannels and intercellular channels are pannexin specific (1). Using the *Xenopus* oocyte model system, Panx1 and Panx1/Panx2, but not Panx2 alone, were discovered to exhibit functionally different hemichannels in single oocytes (1). Similarly, in paired oocytes, Panx1 and Panx1/Panx2 formed homomeric and hetero-meric intercellular channels, respectively, with distinctive func-tional properties (1). In addition, pannexin-based channels showed similar electrical channel properties and sensitivities to the same classes of pharmacologic blockers as connexins (i.e., carbenox-olone; refs. 1, 16). Collectively, the parallel characteristics between connexins and pannexins raise the possibility that aberrant pannexin expression may also occur in cancer cells, and restoration of pannexin expression may revert the transformed phenotype.

Given that Panx1 alone is capable of forming functional channels and its mRNA is endogenously expressed in the brain, it raises a potential correlation between aberrant pannexin expression and glioma tumorigenicity. In this study, we used C6 cells, a well characterized glioma cell line, as our model system. C6 cells are believed to be of astrocytic origin and have been shown to exhibit low connexin43 (Cx43) expression and gap junctional coupling (17, 18). Although Panx1, Panx2, and Panx3 transcripts were present in rat primary astrocytes, none were detected in C6 cells. Restoration of Panx1 expression by stable transfection with either fluorescent- or epitope-tagged Panx1 cDNAs induced a dramatic morphologic change and reversed the neoplastic phenotype of C6 glioma cells. Together, these findings suggest a tumor-suppressive role of Panx1 in C6 glioma cells.

Connexins have been extensively studied in their putative role as tumor suppressors. Pannexins, on the other hand, have just been identified recently and thus far their implication in cancers has not been examined. The present study is the first report on Panx1 as a negative growth regulator and provides insights into novel aspects of gap junctions in cancer research.

Materials and Methods

Cell culture. Primary culture of cortical rat astrocytes and human glioma cell lines (U87, U251, SF188, and SF539) were prepared as described previously (19, 20). C6 glioma cells were obtained from American Type Culture Collection (Manassas, VA) and cultured in DMEM (Invitrogen Corp., Burlington, Ontario, Canada) containing 10% fetal bovine serum, 10 units/mL penicillin, and 10 μg/mL streptomycin at 37°C, 5% CO_2. Stable transfectants were maintained in C6 medium supplemented with 3 μg/mL puromycin (Sigma-Aldrich, St. Louis, MO). Before experimentation, stable transfectants were subcultured into puromycin-free medium.

Total RNA extraction, reverse-transcription-PCR. Total RNA of cultured cells was extracted using Trizol reagent (Invitrogen) and human adult brain total RNA was acquired from Clontech Laboratories, Inc. (Mountain View, CA). Reverse transcription-PCR (RT-PCR) was done as described previously (21). The PCR profile for pannexins was 94°C for 45 s, 50°C (rat) or 58°C (human) for 1 min, and 72°C for 60 s for 35 cycles. Pannexin primer sequences and predicted sizes are listed in Supplementary Table S1. Glyceraldehyde-3-phosphate dehydrogenase (GAPDH) primer sequences and PCR profile were used as described previously (22). Thirty microlites of PCR products and 1 kb DNA ladder (Invitrogen) were simultaneously run on a 1.5% ethidium bromide–stained agarose gel. As a negative control, SuperScript III was replaced with ultrapure MilliQ water to discern false positives of PCR products from DNA-contaminated cDNA products.

Plasmid construction and transfection. Expression vector pRK 5 encoding *Rattus norvegicus Panx1* tagged with c-*myc* (Panx1-myc) or *enhanced green fluorescent protein* (*EGFP*) reporter gene (Panx1-EGFP) were prepared as described previously (16). As a control, AP2 retroviral vector encoding *EGFP* was used (23). The day before transfection, 1×10^6 cells were seeded per 35-mm dish in C6 medium and cotransfected with murine stem cell virus vector encoding a puromycin resistance gene (pMSCVpuro; Clontech Laboratories) and the plasmid of interest (EGFP, Panx1-myc, or Panx1-EGFP) using LipofectAMINE 2000 (Invitrogen) as described previously (19). Cotransfectants were selected with 3 μg/mL puromycin, and clones were subsequently isolated using cloning rings.

Protein isolation and Western blot analysis. Cells were lysed in radioimmunoprecipitation assay (RIPA) buffer containing protease inhibitors (complete, Mini, Roche Diagnostics Corp., Indianapolis, IN) and phosphatase inhibitors (Phosphatase Inhibitor Cocktail 2, Sigma-Aldrich), and DNA was sheared with a 22-gauge needle. Protein concentration was determined by using a bicinchoninic acid (BCA) protein assay kit (Pierce-BioLynx, Brockville, Ontario, Canada). Following boiling for 2 min in SDS sample buffer, 20 μg of total protein and molecular weight standard

(Precision Plus Protein All Blue Standards, Bio-Rad Laboratories, Hercules, CA) were simultaneously subjected to 10% SDS-PAGE and the separated protein bands were transferred onto nitrocellulose membranes. The membranes were blocked with 5% nonfat milk in TBS containing 1% Tween 20 for 1 h and then incubated overnight at 4°C with anti–c-*myc* (mouse; 1:400 dilution; Roche Diagnostics) and anti-GFP antibodies (mouse; 1:1,000 dilution; Stressgen, Ann Arbor, MI). The membranes were immersed in secondary antibody (goat anti-mouse or anti-rabbit IgG-horseradish peroxidase; 1:5,000 dilution; CedarLane Laboratories Ltd., Hornby, Ontario, Canada) for 1 h, incubated with Supersignal (Pierce-BioLynx), and exposed to X-ray film for detection of antibody-bound proteins. As a loading control, the membranes were immunoblotted for GAPDH (mouse, 1:20,000 dilution; CedarLane Laboratories).

Crude membrane fractionation. Cells on a confluent 100-mm plate were harvested into a fractionation solution [10 mmol/L Tris-HCl (pH 7.5), 250 mmol/L sucrose, and protease inhibitors (complete, Mini)]. Samples were then sonicated for 15 s and centrifuged at 30,000 × *g* for 30 min using a TLA120.1 rotor in an Optima TLX Ultracentrifuge (Beckman Coulter, Mississauga, Ontario, Canada). Supernatant (cytoplasmic fraction) was collected and pellet (membrane-enriched fraction) was resuspended in a RIPA buffer supplemented with protease inhibitors (complete, Mini) and phosphatase inhibitors (Phosphatase Inhibitor Cocktail 2) using 22-gauge needles. Protein concentration was determined using a BCA Protein Assay kit.

Immunocytochemistry and live-cell imaging. For live-cell imaging, cells grown on coverslips were washed twice in PBS containing Mg^{2+} and Ca^{2+} and immediately mounted onto glass slides. Samples were viewed under an epifluorescence microscope (Axioplan 2, Carl Zeiss, Toronto, Ontario, Canada) and images were captured using Axiovision (Carl Zeiss). For immunocytochemistry, cells were grown on coverslips, fixed in 4% formaldehyde at room temperature for 10 min, and permeabilized with 0.3% Triton X-100. Plasma membrane and Golgi apparatus were stained with Alexa 594–conjugated wheat germ agglutinin (WGA; 1:200 dilution; Molecular Probes, Eugene, OR) using protocols outlined in the product manual. Nonspecific antibody binding was blocked using 10% bovine serum albumin in PBS and immunolabeled with anti–c-*myc* (mouse; 1:100 dilution; Roche Diagnostics) antibodies for 1 h. Cells were then incubated in Alexa Fluor–conjugated secondary antibodies (goat anti-mouse or anti-rabbit; 1:500 dilution; Molecular Probes) for 1 h and mounted in ProLong Gold antifade with 4′,6-diamidino-2-phenylindole (DAPI, Molecular Probes) onto glass slides. Samples were examined by confocal microscopy (Olympus IX81, Carsen Group, Inc., Markham, Ontario, Canada).

Whole-cell patch-clamp dye loading assay. Coverslips with a confluent layer of cells were placed into artificial cerebrospinal fluid (aCSF) that contained 120 mmol/L NaCl, 26 mmol/L $NaHCO_3$, 3 mmol/L KCl, 1.25 mmol/L NaH_2PO_4, 1.3 mmol/L $MgSO_4$, 2 mmol/L $CaCl_2$, and 10 mmol/L glucose. The aCSF was aerated with 95% O_2/5% CO_2, maintained at 32°C to 34°C with an inline heater, and perfused at a rate of 2 mL/min. Sulforhodamine 101 (SR101) loading was achieved with the whole-cell configuration of the patch-clamp technique using pipettes of 5 to 7 MΩ resistance when loaded with intracellular solution containing 130 mmol/L Kgluconate, 10 mmol/L KCl, 10 mmol/L HEPES, 10 mmol/L EGTA, 1 mmol/L $CaCl_2$, 3 mmol/L MgATP, 0.6 mmol/L Na_2GTP, and 0.01 mmol/L SR101 (pH 7.3).

The membrane under the pipette was disrupted by gentle suction, and SR101 loading of the cell was monitored with confocal microscopy using a Zeiss 510 confocal/multiphoton microscope. SR101 excitation was with a HeNe laser (543 nm). Fluorescence emission was detected by a photomultiplier tube and emitted light filtered (605–660 nm filter). The time constant of dye coupling (τ) was determined by fitting a single exponential to the SR101 fluorescence versus time plot using Clampfit software (Molecular Devices, Sunnyvale, CA). SR101 fluorescence was measured in a user-defined region of interest drawn over the loaded C6 cell and over the first adjacent cell that showed coupling.

Growth curve assay. Cells were seeded in triplicates at 10,000 per well in 12-well plates. C6 medium was replaced every 48 h throughout the

experiment. Day 0 denotes the day of seeding and the number of cells per well was counted on days 1, 3, 4, 6, and 10 using Z1 Coulter Particle Counter (Beckman Coulter) with IsoFlow Sheath Fluid (Coulter Corp., Miami, FL) as a diluent.

Transwell assay. Cells (75,000) were seeded in duplicates at both the top of a transwell insert (BD Biocoat 8.0-μm inserts in 24-well plates, BD Biosciences, Missisagua, Ontario, Canada) and in a separate well without the transwell insert. Cells were incubated for 14 h and subsequently trypsinized from the bottom of the insert (number of traversed cells) and the separately seeded well (number of total cells) for cell counting using Z1 Coulter Particle Counter with IsoFlow Sheath Fluid as a diluent. Cell motility was determined as number of traversed cells per number of total cells.

Soft agar assay. Two-layer soft agar system was used in this assay. Briefly, 2 mL of C6 medium containing 0.6% agar was cast as a bottom layer for each 60-mm plate. Cells were then seeded in triplicates at 10,000 per plate in 2 mL of 0.3% agar medium above the bottom layer. Following 14 days of incubation with fresh medium added every 7 days, samples were stained overnight with 0.01% crystal violet and photographed using AlphaImager 3400 (AlphaInnotech, San Leandro, CA). Colonies were viewed under a microscope (Axioplan 2) and images were captured using Axiovision. The area of each colony was measured and colonies with a size >20,000 μm² were scored as positive. The average area of the colonies was calculated by summing the area of all measured colonies and dividing by the total number of colonies measured. Percentage of colony formation was determined as positive / (positive + negative).

Tumorigenicity assay. Experiments with 6- to 8-week-old female immunodeficient Hsd:athymic nude-*Foxn1*^nu mice (Harlan Sprague-Dawley, Indianapolis, IN) were conducted in the animal facility of the British Columbia Cancer Research Center (Vancouver, British Columbia, Canada). Five mice were used for each sample, and each mouse was inoculated at two sites on the flank/upper hips (500,000 cells per site). Animals were monitored thrice weekly for tumor growth. Tumor volume was calculated according to the equation $L \times W^2 / 2$ with the length (mm) being the longer axis of the tumor. Mice were sacrificed after a combined tumor size of 1,000 mm³ per mouse was reached. All animals were handled under practices and operating procedures complying with the policies of the local animal care committee and the Canadian Council of Animal Care.

Data analysis. Results are expressed as mean ± SE. One-way ANOVA analysis was used for statistical comparisons with $P < 0.05$ considered significant. Each experiment with the exception of the tumorigenicity assay was repeated three or more times with similar results.

Results

Panx1, Panx2, and Panx3 are endogenously expressed in rat primary astrocytes but not in C6 glioma cells. To determine the endogenous pannexin expression in rat primary astrocytes,

Figure 1. Expression of pannexins is absent in C6 glioma cells. *A,* RT-PCR done on total RNA extracted from C6 glioma cells and rat primary astrocytes. C6 cells exhibited no corresponding products for pannexin transcripts. RT-PCR products for Panx1 (185 bp), Panx2 (258 bp), and a less intense band for Panx3 (336 bp) were found in primary astrocytes. *B,* a panel of human gliomas (U87, U251, SF188, and SF539) and human adult brain showed RT-PCR product for Panx1 transcript (195 bp). As a positive control for reverse transcription, bands for GAPDH (515 bp) were detected in all samples. No product was detected when reverse transcriptase (+) was replaced with ultrapure MilliQ water (−).
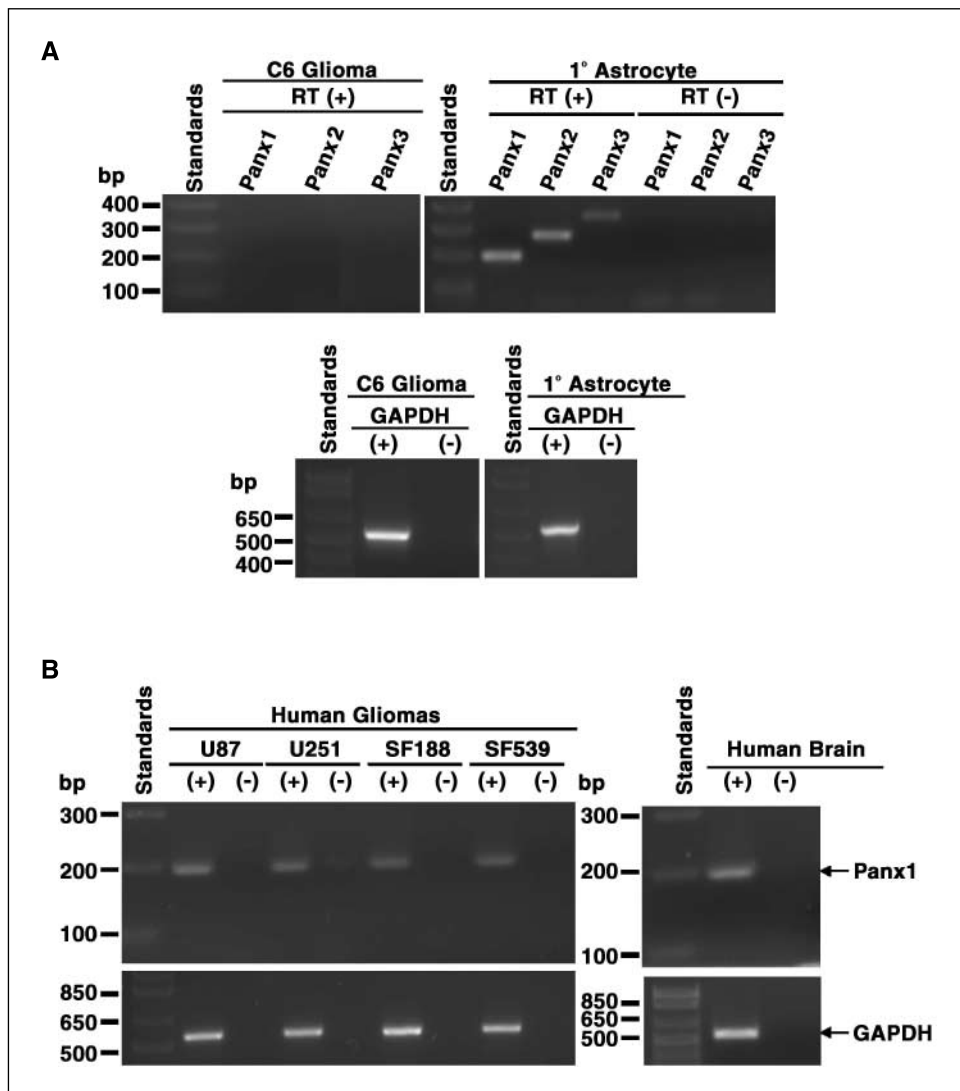
RT-PCR of Panx transcripts was done on total RNA of the astrocytes and showed the presence of Panx1 and Panx2 mRNAs, whereas Panx3 mRNA was detected as a less intense band (Fig. 1*A*). To ensure the purity of primary astrocyte cultures, expression of glial fibrillary acidic protein (GFAP), a common astrocytic marker, was examined by immunocytochemistry; >99% of the cells exhibited GFAP signal. However, when we tested the tumorigenic counterpart, rat C6 gliomas, no mRNAs for any of the pannexins were detected (Fig. 1*A*). Human adult brain and a panel of human glioma cell lines (U87, U251, SF188, and SF539) were also studied and Panx1 mRNA was detected (Fig. 1*B*). Because Panx1 transcript is present in rat primary astrocytes but not in C6 glioma cells, we hypothesized that Panx1 may act as a tumor suppressor once its expression is restored.

Stable Panx1-transfected C6 cells express transfected pannexin cDNAs. To verify translational expression of transfected cDNAs in the stable C6 transfectants, Western blot analysis was done. We generated several clones for each type of transfectant with varying expression levels (Fig. 2*A*). From them, we selected the following clones for further experimentation: EGFP clones 5 and 15,

Panx1-myc clones 6 and 19, and Panx1-EGFP clones 2 and 8. Using EGFP clone 5, Panx1-myc clone 19, and Panx1-EGFP clone 2, we showed corresponding protein bands for each transfected cDNA at the predicted product sizes using either anti-GFP or anti–c-*myc* antibody, confirming the specificity of protein expression (Fig. 2*B*).

Panx1 expression induces cellular morphologic change. Cellular morphology of stable Panx1-expressing C6 cells was studied by live-cell imaging (Fig. 2*C*). This technique was used as it preserves the cellular morphology without the artifacts induced by conventional fixation processes. GFP signals positively identified expression of the stable transfectants (Fig. 2*C, d* and *g*). Control (EGFP; Fig. 2*C, e*) showed a spindle-shaped morphology, which is typical of normal C6 cells (Fig. 2*C, b*). By contrast, Panx1-EGFP (Fig. 2*C, h*) displayed a flattened cell morphology. Additionally, whereas typical EGFP expression was found throughout the cytoplasm in the control transfectants (Fig. 2*C, d* and *f*), Panx1-EGFP was prominently observed in the perinuclear and peripheral regions of the cells (Fig. 2*C, g* and *i*).

Cellular localization pattern of Panx1. To further investigate the subcellular localization of Panx1 and the resultant
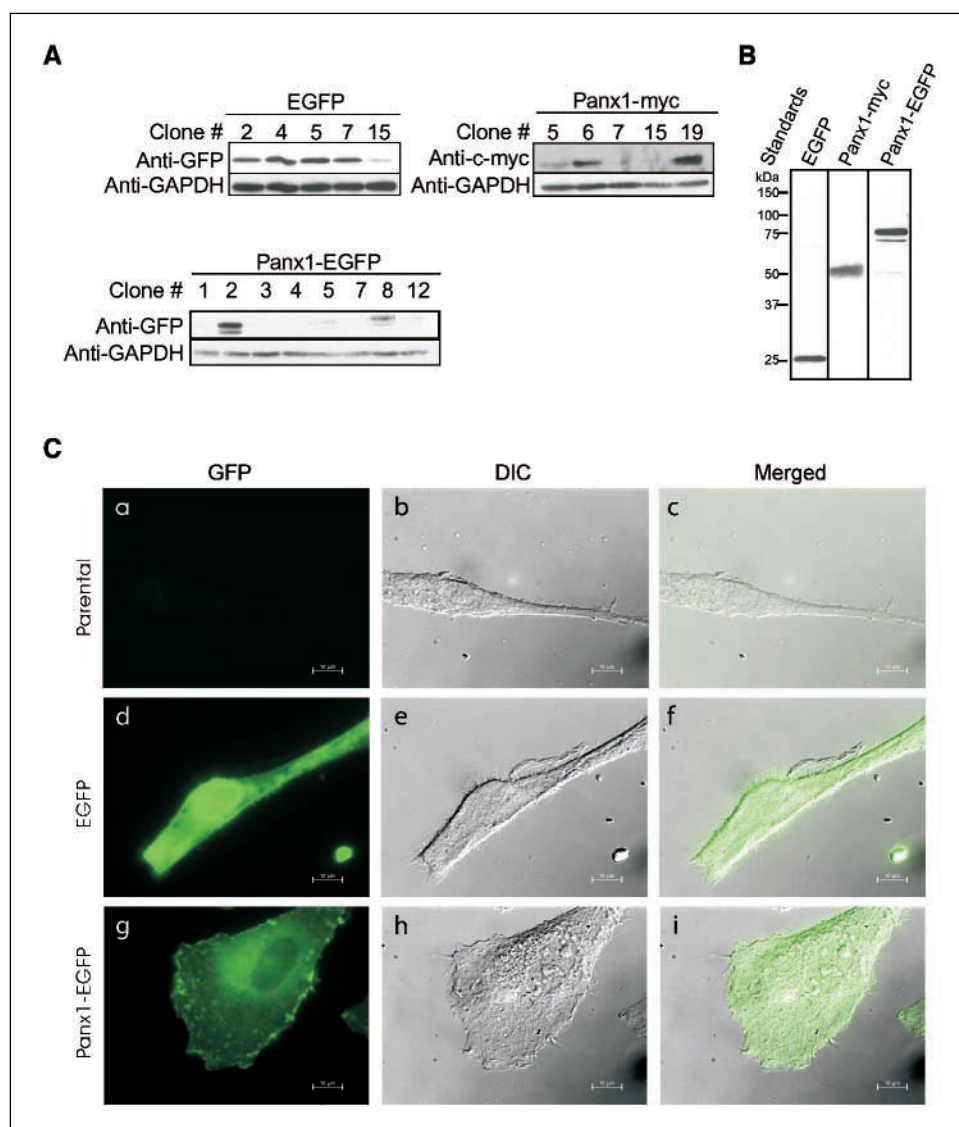
Figure 2. Expression and altered cellular morphology in stable Panx1-transfected C6 glioma cells. *A*, Western blot analysis of several stable EGFP- and Panx1-transfected C6 clones. Protein expression in various clones was determined using corresponding antibodies against GFP and c-*myc*. *B*, sample immunoblots showing protein expression in selected stable C6 transfectants at predicted sizes (EGFP, 25 kDa; Panx1-myc, 50 kDa; and Panx1-EGFP, 73 kDa). GAPDH was probed with anti-GAPDH antibody as a loading control. *C*, live-cell imaging revealing cellular morphology of parental (*a–c*), stable control (EGFP; *d–f*), and Panx1-EGFP (*g–i*) C6 transfectants. Differential interference contrast (*DIC*) images of Panx1-EGFP–transfected C6 cells (*h*) exhibited a flattened morphology when compared with the control (*e*). Morphology of parental C6 cells (*b*) seemed to be similar to that of stable EGFP transfectants (*e*). *Bar,* 10 μm.

Figure 3. Cellular localization of Panx1 and altered membrane morphology in stable Panx1-transfected C6 glioma cells. *A,* immunocytochemistry for stable control (EGFP; *a–c*) and Panx1-EGFP (*d–f*) transfectants. Expression is shown by GFP fluorescence (*a* and *d*); Golgi apparatus and plasma membrane (*b* and *e*) were stained with WGA. Nuclei are visualized by DAPI in merged images (*c* and *f*). Panx1-EGFP seemed to localize to the perinuclear region (*arrowheads*) and cell membrane (*arrows*). *Bar,* 30 μm. *B,* Western blot analysis showing that Panx1-EGFP is predominantly associated with the membrane fraction. Whereas EGFP expression of the control transfectant was identified in the cytosol fraction (*C*), Panx1-EGFP was only detected in membrane-enriched fractions (*M*). Probing with anti-GAPDH antibody showed traces of GAPDH in the membrane-enriched fractions when compared with the cytosol fractions.
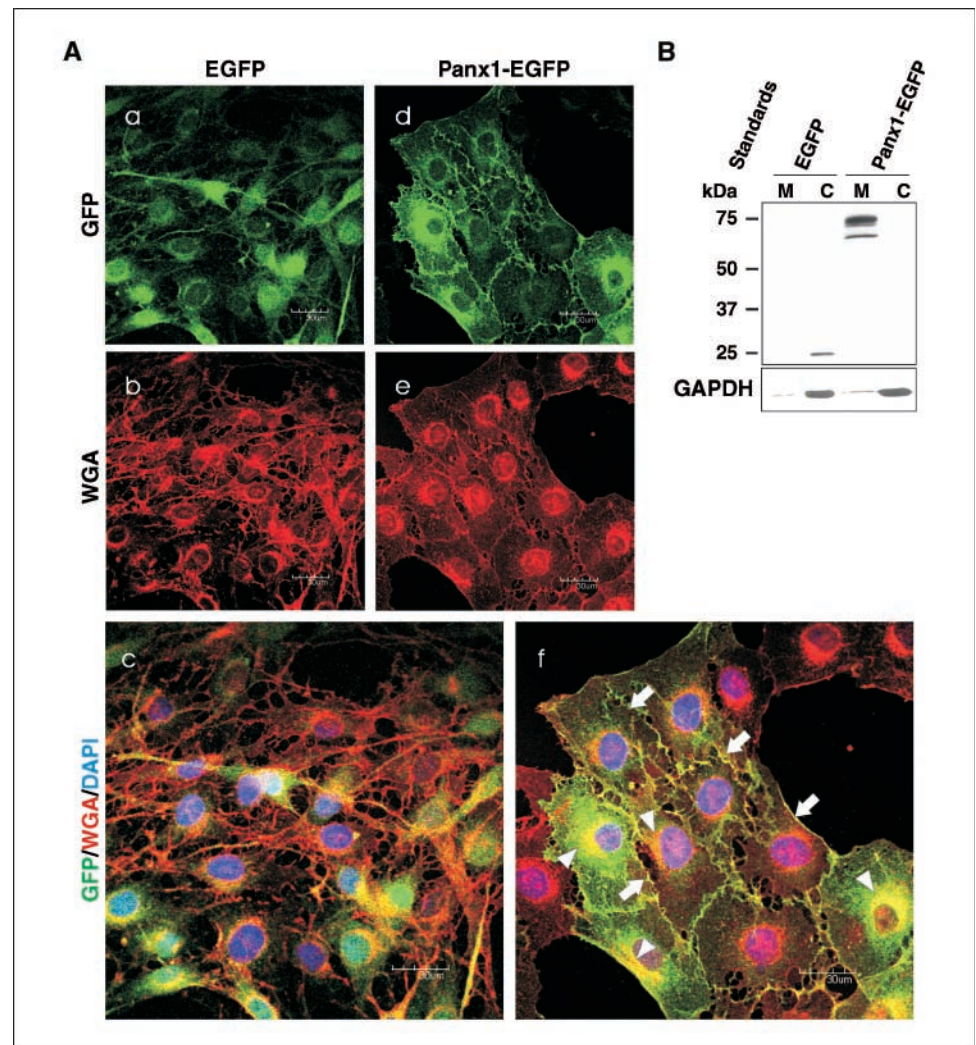
morphologic change observed by live-cell imaging (Fig. 2*C*), direct fluorescent labeling of the Golgi apparatus and plasma membrane using Alexa 568–conjugated WGA was done (24), and samples were examined using confocal microscopy. Panx1-EGFP was localized predominately at the cell membrane as well as to the perinuclear region (Fig. 3*A, f*) as anticipated because Panx1 is a transmembrane protein. Conversely, control cells expressing only EGFP displayed fluorescence throughout the entire cytoplasm, a typical expression pattern found in GFP transfectants (Fig. 3*A, c*; ref. 25). This correlates with our finding from the live-cell imaging experiment (Fig. 2*C*): whereas the control cells retained the spindle-shaped characteristic of C6 cells, Panx1-EGFP cells displayed a flattened morphology, which is clearly revealed on the plasma membrane staining (Fig. 3*A*). To verify the observed Panx1-specific localization pattern, Western blot analysis on cytoplasmic and membrane-enriched fractionations was carried out (Fig. 3*B*). As expected, EGFP expression was only detected in the cytosol fraction. By contrast, Panx1-EGFP expression was only found in the membrane-enriched fraction, which includes the Golgi apparatus and plasma membrane, concurring with the above findings. Using the anti-GAPDH antibody, we observed limited, but not appreciable amounts of this protein in the membrane-enriched fractions. To control for possible effects

contributed by the *EGFP* reporter gene, the experiments were also conducted using stable C6 Panx1-*myc* transfectants, and similar results were found (data not shown).

Panx1 expression increases dye coupling in C6 cells. As both Panx1-myc and Panx1-EGFP localize to the cell membrane, we hypothesize that functional Panx1-based channels might be present, yielding an increase in gap junctional coupling in the Panx1-expressing cells. Using the whole-cell patch-clamp loading assay with SR101, a fluorescent dye that labels astrocytic networks and passes through presumptive Panx1 neuronal hemichannels (26, 27), the Panx1 transfectants exhibited a significant increase in dye transfer when compared with the control (EGFP only; Fig. 4*A* and *B*). Panx1-expressing transfectants were strongly coupled to at least one neighbor, but weaker coupling to additional neighbors was also observed (Fig. 4*A*). In addition, the SR101 fluorescence increase in the control cells occurred with a slow time constant (τ), $\tau = 1,153 \pm 379.2$ s ($n = 5$) and increased to only <5% above the background (Fig. 4*C*). The time constant of dye coupling for Panx1-expressing cells was significantly faster when compared with the control cells [Panx1-EGFP, 238.7 ± 99.4 s ($n = 9$); Panx1-myc, 230.5 ± 41.3 s ($n = 7$); τ was not significantly different between Panx1-EGFP and Panx1-myc cells; Fig. 4*C*].
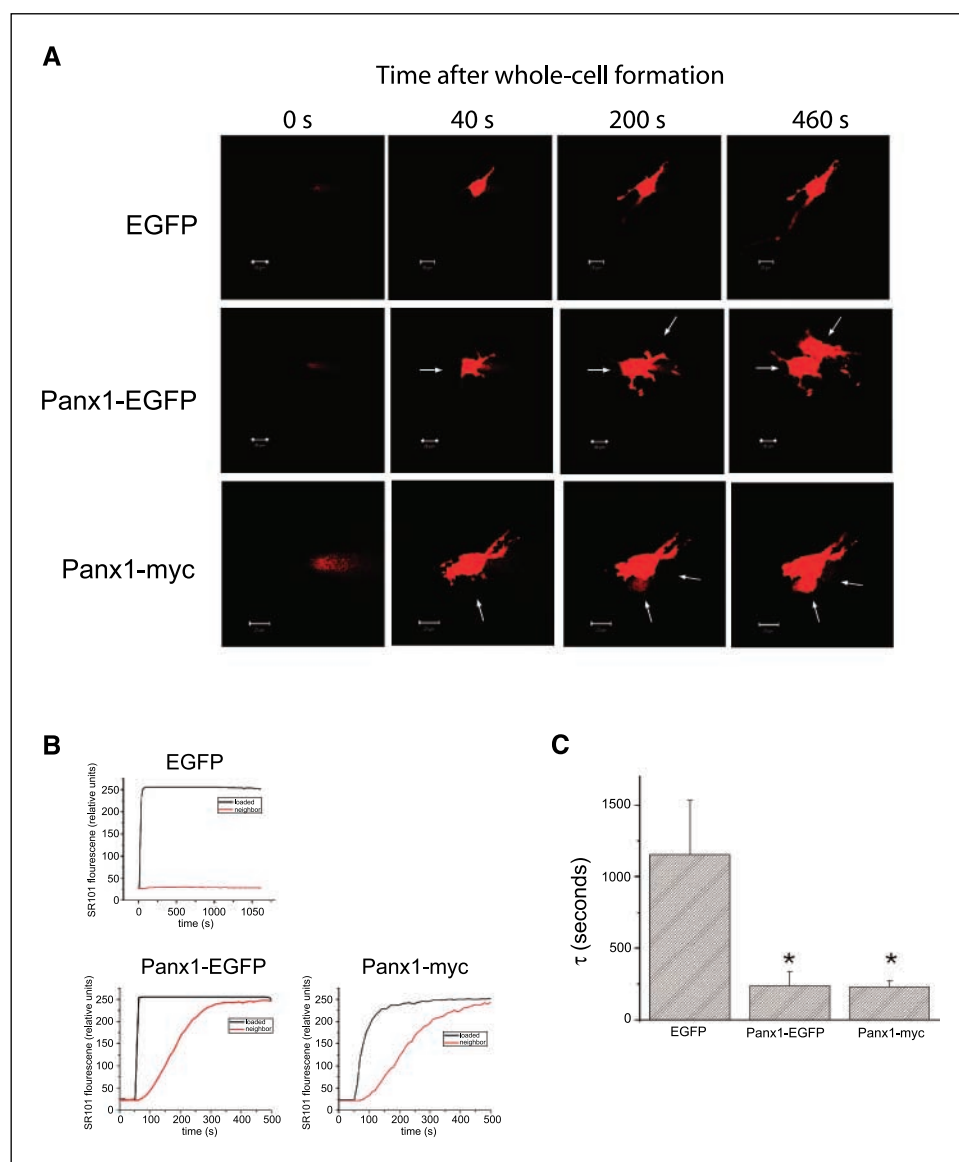
Figure 4. Dye coupling in C6 Panx1 transfectants is observed following intracellular loading with a patch pipette. *A,* donor cells from the transfectants indicated were loaded with 10 μmol/L SR101 (*red*) via the whole-cell configuration of the patch-clamp technique. No significant dye coupling was observed in control cells (*top row*). By contrast, Panx1 transfectants showed dye transfer to neighboring cells (*arrows*) following loading of the donor cell (*middle and bottom rows*). EGFP, 5 of 11 cells with weak coupling; Panx1-EGFP, 9 of 10 cells with stronger coupling; and Panx1-myc, 7 of 9 cells with stronger coupling. *B,* time course of SR101 intensity inside dye-loaded cells and neighboring cells. *C,* the SR101 fluorescence increase in the control cells occurred with a significantly slower time constant when compared with the Panx1 transfectants. *, $P < 0.05$.

Panx1 expression suppresses the transformed phenotype of C6 cells. Proliferation properties were first examined using the growth curve assay. A significant decrease in growth rate was evident in both stable tagged Panx1 transfectants when compared with the control cells starting from day 3 (Fig. 5*A*). The reduced growth rate was continually observed up to day 6, which coincided with the confluence of the cultures. In addition, stable Panx1 transfectants displayed a significant decrease in saturation density, as revealed by counting cells postconfluence (days 6–10). Furthermore, samples set up in parallel to the growth curve experiments showed no apparent increase in the percentage of DAPI-stained apoptotic nuclei in the stable Panx1 transfectants (data not shown).

Aberration in cellular morphology often associates with changes in motility and invasiveness of cancer cells (28). As Panx1 expression induces a distinctive morphologic change from the typical spindle shape to the flattened morphology (Fig. 2*C*), it suggests that Panx1 may also affect the motility of the glioma cells. To examine this possibility, transwell assays were carried out and a

significant decrease in cell motility was observed in the Panx1 transfectants when compared with the control (Fig. 5*B*). The assays were completed in 14 h, which is less than the doubling time of C6 cells (~16 h; ref. 29).

Another hallmark of the transformed phenotype is anchorage-independent growth. To assess this, we did soft agar assays and found a significant decrease in the percentage of colony formation in the Panx1 transfectants compared with the control (Fig. 6*B*). Similarly, numerous large colonies (>100,000 μm²) were readily detected in the control samples, which is far greater than the average size of both Panx1-myc and Panx1-EGFP colonies (Fig. 6*A*). Intriguingly, Panx1-EGFP samples consistently showed a greater average area of colonies and percentage of colony formation than that of Panx1-myc ($P < 0.001$; Fig. 6*A*).

Finally, tumorigenicity assays were done to examine tumor-suppressive effects of Panx1 *in vivo*. All of the injected sites from the control and Panx1 transfectants developed tumors. When compared with the control, a significant reduction of average tumor size was found in both tagged Panx1-expressing cells

starting from days 12 to 16. By day 16, the mice injected with the control cells were sacrificed as the tumor size per mouse had exceeded 1,000 mm^3 (Fig. 6*C*).

Discussion

In the past, connexins have been considered the sole mammalian gap junctional proteins. Using the *Xenopus* oocyte system, studies have shown formation of functional hemichannels and intercellular channels by Panx1 and Panx1/Panx2, implicating that pannexin-based channels may play important physiologic roles in mammalian cells (1). In view of the functional similarity with connexins, for which an inverse relationship between gap junctions and tumor progression has long been suggested (10), we sought to examine the possible correlation between aberrant pannexin expression and tumorigenicity in gliomas by using the C6

glioma cell model. We have shown that Panx1, Panx2, and Panx3 transcripts are expressed in primary astrocytes but not in its tumorigenic counterpart, C6 glioma cells. Induction of Panx1 expression by gene transfection revealed a unique Panx1 localization pattern and elicited a dramatic morphologic change in Panx1-expressing cells. Using the whole-cell patch-clamp loading assay with SR101, a significant increase in dye coupling was discovered in Panx1-expressing cells. Moreover, stable Panx1 expression consistently suppressed proliferation both *in vitro* and *in vivo*. These findings provide strong evidence that Panx1 mediates tumor suppressive effects in C6 glioma cells via the functional Panx1-based intercellular channels.

To date, protein expression of pannexins has not been fully defined in mammals due to the lack of specific antibodies. Nevertheless, through Northern blot analysis and *in situ* hybridization experiments in rats, pannexin mRNA expression was reported to be location specific (1, 5, 30). As Panx1 and Panx2 mRNAs are present in rat brain at P1, we anticipated that primary astrocytes would possess both transcripts (5, 30). Albeit Panx3 distribution has not been extensively studied, previous reports have suggested low Panx3 mRNA expression in the brain as well as in osteoblasts and synovial fibroblasts as shown by expressed sequence tag data (1, 3, 31). Whereas a previous study by Vogt et al. (5) using *in situ* hybridization shows Panx1 (in hippocampus) and Panx2 (in cerebral cortex) expression in neuronal but not astrocytic cells of postnatal rat brain, we positively identified both of these pannexin mRNAs in primary astrocytes. These differences could be attributed to the reactive-like nature of newly cultured astrocytes, a distinct population of astrocytes extracted from the neonatal cortex, and/or increased sensitivity of PCR analysis in detecting pannexin mRNAs over the *in situ* hybridization technique (32). Additionally, we used cultures, in which >99% of primary astrocytes were GFAP positive, to avoid possible false-positive observations as a result of neuronal and/or fibroblastic cell contaminations. We also observed a less intense band for Panx3 in the primary astrocytes, which agrees with the previous study that Panx3 is present in the brain as a very low-level transcript (3). The absence of pannexin transcripts in C6 cells implicates the loss or down-regulation of *Panx* genes during tumor transformation. Similarly, down-regulation or absence of connexin expression, including Cx43 in C6 cells, has been reported in various types of neoplastic cells (18, 33–35). Because pannexins are gap junctional proteins, such a relationship could also hold true for the pannexins, suggesting their possible tumor-suppressive role.

Interestingly, Panx1 transcript was detected in a panel of human glioma cell lines (U87, U251, SF188, and SF539) and human adult brain. Because Panx1 is ubiquitously expressed, it was expected to be observed in the brain and used as a positive control. The presence of Panx1 mRNA in the human gliomas, in contrast to the C6 cells, could indicate that the loss of Panx1 transcript specifically apply to a subset of gliomas. Nevertheless, aberrant pannexin expression may also occur at the translational level, resulting in tumor transformation. Further examination of Panx1 protein expression is needed to test this supposition.

As Panx1 expression has been shown in primary astrocytes and, unlike Panx2, has been reported to readily form functional channels, the present study focused on the possible tumor-suppressive roles of Panx1 in C6 cells (1). Because a specific anti-Panx1 antibody is currently unavailable for the identification of positive Panx1-transfected cells, clones were generated from stable transfection with Panx1-myc and Panx1-EGFP cDNAs. Both types
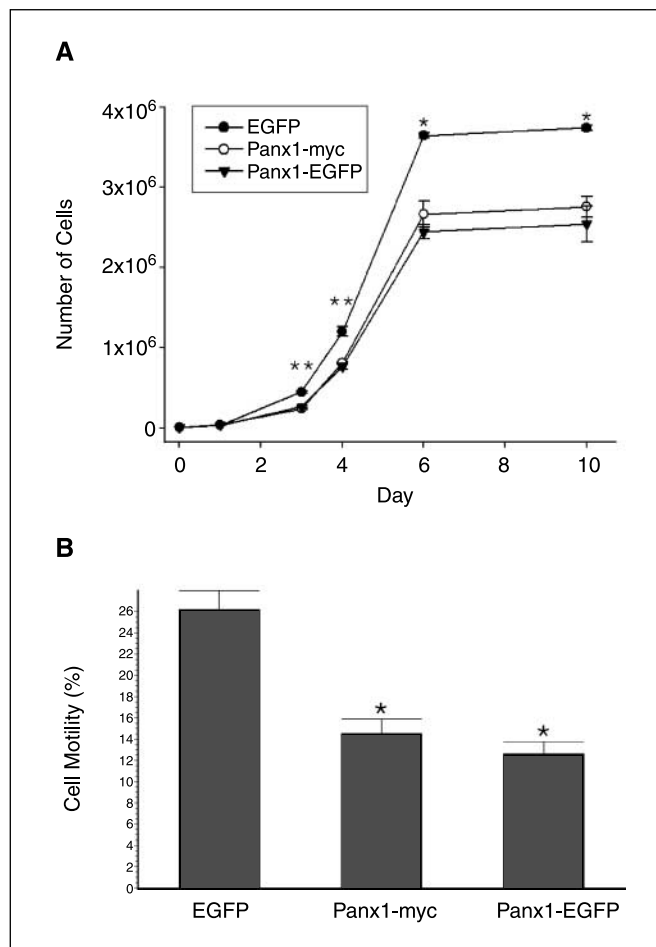
Figure 5. Panx1 expression reduces C6 cell proliferation, saturation density, and motility. *A,* growth curve assay of the control (EGFP) and stable tagged Panx1 transfectants (myc or EGFP). Cells were seeded at 10,000 per well in 12-well plates. Day 0 denotes the day of seeding and the number of cells per well was counted on days 1, 3, 4, 6, and 10 with C6 medium replaced every 48 h. A significant reduction in the growth rates of the Panx1-transfected C6 cells was observed when compared with the control (EGFP) beginning on days 3 to 4. **, *P* < 0.001 for Panx1 transfectants compared with control. This reduced growth rate was consistently observed into day 6. *, *P* < 0.01 for Panx1 transfectants compared with control. A significant decrease in saturation density of the Panx1 transfectants was also evident from day 6 to day 10. *B,* transwell assay exhibiting a significant reduction in cell motility of the Panx1 transfectants (Panx1-myc, 14.44 ± 1.308%; Panx1-EGFP, 12.54 ± 1.106%) when compared with the control (EGFP, 25.99 ± 1.792%). *, *P* < 0.001.
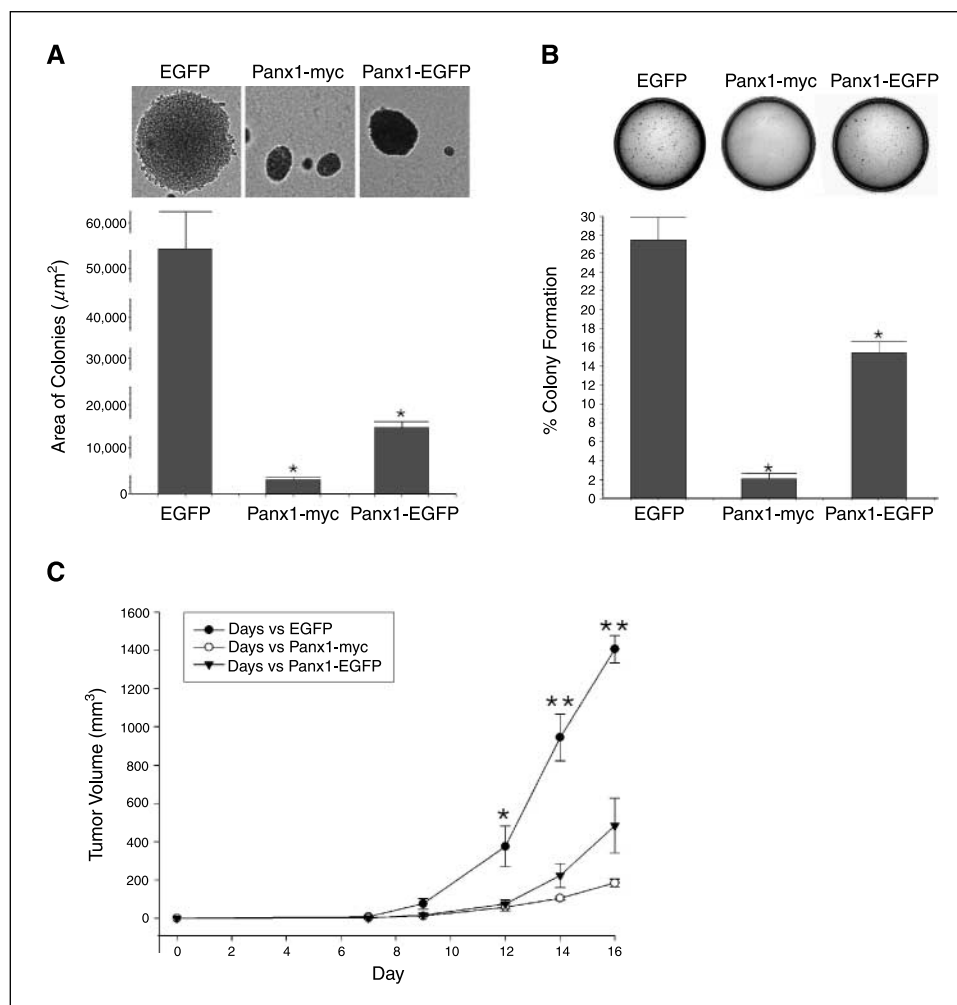
Figure 6. Panx1 expression suppresses anchorage-independent growth and *in vivo* tumor formation in C6 glioma cells. *A, top,* appearance of individual colonies of each stable transfectant in the soft agar. Note that whereas large colonies were readily detected in the control (EGFP, 54,358 ± 8,144 µm^2), Panx1 transfectants exhibited fewer and smaller colonies (Panx1-myc, 3,107.84 ± 585.86 µm^2; Panx1-EGFP, 14,706.05 ± 1,226.0 µm^2). *B, top,* sample plates from soft agar assay showing an overall reduction of colony formation in stable Panx1 transfectants (Panx1-myc, 2.03 ± 0.65%; Panx1-EGFP, 15.70 ± 1.13%) when compared with the control (EGFP, 27.89 ± 2.486%). On quantification and statistical analysis, Panx1 transfectants showed a significant decrease in both the average area of colonies (*A*) and the efficiency of colony formation (*B*). *, $P < 0.001$ compared with control. *C,* tumorigenicity assay of stable Panx1 transfectants. Day 0 denotes the day of injection. A significant reduction in the tumor size of the Panx1-transfected C6 cells was observed when compared with the control (EGFP) beginning on day 12 and consistently observed into day 16. *, $P < 0.05$; **, $P < 0.001$. Mice injected with the Panx1-expressing cells only reached similar tumor size as the control on day 16 until an average of 6 d later (Panx1-myc, five of five mice on day 23; Panx1-EGFP, three of five mice on day 19 and two of five mice on day 23).

of stable transfectant were used in all experiments wherever possible to verify the findings, and similar properties induced by Panx1 expression were found throughout the study. Additionally, more than one clone from each type of stable transfectants was used to minimize clonal variation. Furthermore, Cx43 was examined to ensure similar expression levels between the selected clones to avoid Cx43-elicited effects in this study (data not shown).

In the stable tagged Panx1 transfectants, transfected cDNAs were successfully expressed and the protein prominently localized to the perinuclear Golgi apparatus and plasma membrane. Because Panx1 has a predicted topology resembling connexins, as well as reported channel-forming ability, it is expected that Panx1 is localized to the plasma membrane (1, 15). Moreover, the unique localization pattern of Panx1 to the perinuclear Golgi apparatus and plasma membrane seemed to be similar to that of connexin26 (Cx26) and Cx43 expression (25, 36). Previous studies have revealed a protein trafficking pathway shared by Cx26 and Cx43 where both proteins are transported through the Golgi apparatus before being translocated to the membrane (36–38). Although it is beyond the scope of this study, our current findings suggest that Panx1 may be trafficked in a similar pathway as the connexins and thus warrants future investigation.

Coinciding with Panx1 expression at the plasma membrane, Panx1 transfectants displayed a flattened morphology and reduced cell motility. When Cx43 was overexpressed in C6 cells, actin stressed fibers were induced and a flattened morphology along with an increase in gap junctional coupling were observed (13, 39). Since then, various studies have shown direct interactions between connexins and other junctional proteins, including zonula occludens-1 (tight junction) and cadherins (adherens junction), suggesting gap junctions as an anchorage site for the cytoskeleton on the plasma membrane (40). Furthermore, innexin2 (Inx2) and innexin 3 have also been shown to colocalize with components of the adherens junction in *Drosophila* (6). Specifically, a recent study by Lehmann et al. (41) has shown that Inx2 directly interacts with DE-cadherin and β-catenin. Together with our current findings and previous literature, we hypothesize that Panx1 may interact with tight and/or adherens junctional proteins and hence contributed to the observed flattened morphology and reduced cell motility via cytoskeletal reorganization.

A significant reduction of cell proliferation and saturation density was clearly evident in the stable Panx1 transfectants. In addition, the reductions observed were not a result of cell death, as samples set up in parallel to the growth curve experiment showed no apparent increase in the percentage of apoptotic nuclei (data not shown). These *in vitro* results are further strengthened by the *in vivo* tumorigenicity assay. As Panx1 expression was found at the plasma membrane and formed a structural pattern resembling Cx43 at the cell membrane between cell contacts, we were

interested in determining whether functional Panx1 intercellular channels were present (19, 42). Loading Panx1-expressing cells via dialysis from a patch-pipette with SR101, a fluorescent dye, showed a significant increase in coupling when compared with the control. This novel discovery suggests that, similar to Cx43, Panx1 forms functional intercellular channels when stably expressed in C6 cells and mediates tumor-suppressive effects (13).

Nevertheless, the effects induced by Panx1 expression may also be dependent on electrical as well as biochemical coupling (1, 2). Like connexins, Panx1 may exert its effects via intra-cellular signaling pathways without direct communication with neighboring cells (10). Increasing evidence indicates that the tumor-suppressive effects of connexins may be unrelated to functional gap junctions and are instead a result of interplay with intracellular signaling pathways (10). The present study shows that Panx1 expression induces a dramatic morphologic change, implying that molecular targets other than gap junctional coupling are affected. Another piece of evidence support-ing this notion is derived from the soft agar assays. In the assay, single cells are seeded into soft agar and are therefore devoid of cell-cell communication in the initial stage of colony develop-ment. Consistently, the Panx1 transfectants exhibited a signifi-cant decrease in the percentage of colony formation, suggesting a gap junction–independent effect of Panx1. From the same assay, we also found a significant reduction in the average size of colonies. In agreement with the dye coupling data, this could implicate a gap junction–dependent role of pannexin-based channels during the later stages of colony development as multiple cells become available for cell-cell communication. Collectively, our findings suggest that Panx1 may act both gap junction dependently and independently to elicit tumor suppression.

Albeit not statistically significant in all experiments, Panx1-myc consistently exhibited a stronger tumor-suppressive phenotype than Panx1-EGFP both *in vitro* and *in vivo*. As tagged Panx1 forms hemichannels less efficiently than untagged Panx1, we speculate that the difference could be attributed to the different tags; because EGFP yields a greater sized protein, it may hinder the normal conformation of Panx1 protein and in turn affect Panx1 functionality more readily than the c-*myc* tag, resulting in the more prominent tumor-suppressive phenotype seen in stable Panx1-myc transfectants.

Although connexins have been shown to modulate glioma cell proliferation and tumorigenesis, tumor-suppressive implications of pannexins have not been investigated. To our knowledge, this is the first study that shows a direct correlation between aberrant Panx1 expression and tumorigenicity. In the present study using C6 glioma cells, we clearly showed that restoration of Panx1 expression induces tumor suppression. It would be of great interest to examine if a reduction in pannexin expression occurs in other types of cancer. Similar to connexins, a recent report has also shown K(v)ss3 to be a potential regulator of Panx1, implicating that pannexins can be regulated through protein interactions (43). Although many agents have been reported to suppress tumors by up-regulating connexins and GJIC, it is possible that such agents could also regulate pannexin expression (44). The model cell system described here can be used for further studies on the molecular mechanisms underlying the phenotypes and effects elicited by Panx1 overexpression.

Acknowledgments

References

1. Bruzzone R, Hormuzdi SG, Barbe MT, Herb A, Monyer H. Pannexins, a family of gap junction proteins expressed in brain. Proc Natl Acad Sci U S A 2003;100: 13644–9.
2. Bao L, Locovei S, Dahl G. Pannexin membrane channels are mechanosensitive conduits for ATP. FEBS Lett 2004;572:65–8.
3. Baranova A, Ivanov D, Petrash N, et al. The mamma-lian pannexin family is homologous to the inverte-brate innexin gap junction proteins. Genomics 2004; 83:706–16.
4. Sasakura Y, Shoguchi E, Takatori N, et al. A genome-wide survey of developmentally relevant genes in Ciona intestinalis. X. Genes for cell junctions and extracellular matrix. Dev Genes Evol 2003;213:303–13.
5. Vogt A, Hormuzdi SG, Monyer H. Pannexin1 and Pannexin2 expression in the developing and mature rat brain. Brain Res Mol Brain Res 2005;141:113–20.
6. Bauer R, Loer B, Ostrowski K, et al. Intercellular communication: the *Drosophila* innexin multiprotein family of gap junction proteins. Chem Biol 2005;12:515–26.
7. Barbe MT, Monyer H, Bruzzone R. Cell-cell commu-nication beyond connexins: the pannexin channels. Physiology (Bethesda) 2006;21:103–14.
8. Simon AM, Goodenough DA. Diverse functions of vertebrate gap junctions. Trends Cell Biol 1998;8:477–83.
9. Loewenstein WR. The cell-to-cell channel of gap junctions. Cell 1987;48:725–6.
10. Naus CC. Gap junctions and tumour progression. Can J Physiol Pharmacol 2002;80:136–41.
11. Mesnil M. Connexins and cancer. Biol Cell 2002;94: 493–500.
12. Naus CC, Elisevich K, Zhu D, Belliveau DJ, Del Maestro RF. *In vivo* growth of C6 glioma cells trans-fected with connexin43 cDNA. Cancer Res 1992;52: 4208–13.
13. Zhu D, Caveney S, Kidder GM, Naus CC. Transfection of C6 glioma cells with connexin 43 cDNA: analysis of expression, intercellular coupling, and cell proliferation. Proc Natl Acad Sci U S A 1991;88:1883–7.
14. Trosko JE, Ruch RJ. Gap junctions as targets for cancer chemoprevention and chemotherapy. Curr Drug Targets 2002;3:465–82.
15. Panchin YV. Evolution of gap junction proteins-the pannexin alternative. J Exp Biol 2005;208:1415–9.
16. Bruzzone R, Barbe MT, Jakob NJ, Monyer H. Pharmacological properties of homomeric and hetero-meric pannexin hemichannels expressed in *Xenopus* oocytes. J Neurochem 2005;92:1033–43.
17. Barth RF. Rat brain tumor models in experimental neuro-oncology: the 9L, C6, T9, F98, RG2 (D74), RT-2, and CNS-1 gliomas. J Neurooncol 1998;36:91–102.
18. Naus CC, Bechberger JF, Caveney S, Wilson JX. Expression of gap junction genes in astrocytes and C6 glioma cells. Neurosci Lett 1991;126:33–6.
19. Ozog MA, Bernier SM, Bates DC, Chatterjee B, Lo CW, Naus CC. The complex of ciliary neurotrophic factor-ciliary neurotrophic factor receptor α up-regu-lates connexin43 and intercellular coupling in astrocytes via the Janus tyrosine kinase/signal transducer and activator of transcription pathway. Mol Biol Cell 2004; 15:4761–74.
20. Naus CC, Bechberger J, Bond SL. In: Spray DC, Dermietzel R, editors. Gap junctions in the nervous systems. Georgetown: R.G. Landes Co.; 1996. p. 193–9.
21. Ozog MA, Bechberger JF, Naus CC. Ciliary neuro-trophic factor (CNTF) in combination with its soluble receptor (CNTFRα) increases connexin43 expression and suppresses growth of C6 glioma cells. Cancer Res 2002;62:3544–8.
22. Yang CW, Lim SW, Han KW, et al. Upregulation of ciliary neurotrophic factor (CNTF) and CNTF receptor α in rat kidney with ischemia-reperfusion injury. J Am Soc Nephrol 2001;12:749–57.
23. Mao AJ, Bechberger J, Lidington D, Galipeau J, Laird DW, Naus CC. Neuronal differentiation and growth control of neuro-2a cells after retroviral gene delivery of connexin43. J Biol Chem 2000;275: 34407–14.
24. Kovacs WJ, Schrader M, Walter I, Stangl H. The hypolipidemic compound cetaben induces changes in Golgi morphology and vesicle movement. Histochem Cell Biol 2004;122:95–109.
25. Falk MM. Connexin-specific distribution within gap junctions revealed in living cells. J Cell Sci 2000;113: 4109–20.
26. Nimmerjahn A, Kirchhoff F, Kerr JN, Helmchen F. Sulforhodamine 101 as a specific marker of astroglia in the neocortex *in vivo*. Nat Methods 2004;1:31–7.
27. Thompson RJ, Zhou N, MacVicar BA. Ischemia opens neuronal gap junction hemichannels. Science 2006;312: 924–7.
28. Etienne-Manneville S, Hall A. Rho GTPases in cell biology. Nature 2002;420:629–35.

29. Zhu D, Kidder GM, Caveney S, Naus CC. Growth retardation in glioma cells cocultured with cells over-expressing a gap junction protein. Proc Natl Acad Sci U S A 1992;89:10218–21.

30. Ray A, Zoidl G, Weickert S, Wahle P, Dermietzel R. Site-specific and developmental expression of pannexin1 in the mouse nervous system. Eur J Neurosci 2005;21:3277–90.

31. Panchin Y, Kelmanson I, Matz M, Lukyanov K, Usman N, Lukyanov S. A ubiquitous family of putative gap junction molecules. Curr Biol 2000;10:R473–4.

32. Wu VW, Schwartz JP. Cell culture models for reactive gliosis: new perspectives. J Neurosci Res 1998;51:675–81.

33. Laird DW, Fistouris P, Batist G, et al. Deficiency of connexin43 gap junctions is an independent marker for breast tumors. Cancer Res 1999;59:4104–10.

34. Tsai H, Werber J, Davia MO, et al. Reduced connexin 43 expression in high grade, human prostatic adeno-carcinoma cells. Biochem Biophys Res Commun 1996; 227:64–9.

35. Sawey MJ, Goldschmidt MH, Risek B, Gilula NB, Lo CW. Perturbation in connexin 43 and connexin 26 gap-junction expression in mouse skin hyperplasia and neoplasia. Mol Carcinog 1996;17:49–61.

36. Thomas T, Jordan K, Simek J, et al. Mechanisms of Cx43 and Cx26 transport to the plasma membrane and gap junction regeneration. J Cell Sci 2005;118:4451–62.

37. Laird DW, Castillo M, Kasprzak L. Gap junction turnover, intracellular trafficking, and phosphorylation of connexin43 in brefeldin A-treated rat mammary tumor cells. J Cell Biol 1995;131:1193–203.

38. Musil LS, Goodenough DA. Multisubunit assembly of an integral plasma membrane channel protein, gap junction connexin43, occurs after exit from the ER. Cell 1993;74:1065–77.

39. Naus CC, Zhu D, Todd SD, Kidder GM. Character-istics of C6 glioma cells overexpressing a gap junction protein. Cell Mol Neurobiol 1992;12:163–75.

40. Giepmans BN. Gap junctions and connexin-interacting proteins. Cardiovasc Res 2004;62:233–45.

41. Lehmann C, Lechner H, Loer B, et al. Heteromeriza-tion of innexin gap junction proteins regulates epithelial tissue organization in *Drosophila*. Mol Biol Cell 2006;17: 1676–85.

42. Fu CT, Bechberger JF, Ozog MA, Perbal B, Naus CC. CCN3 (NOV) interacts with connexin43 in C6 glioma cells: possible mechanism of connexin-mediated growth suppression. J Biol Chem 2004;279:36943–50.

43. Bunse S, Haghika A, Zoidl G, Dermietzel R. Identification of a potential regulator of the gap junction protein pannexin1. Cell Commun Adhes 2005; 12:231–6.

44. Dhein S. Gap junction channels in the cardiovascular system: pharmacological and physiological modulation. Trends Pharmacol Sci 1998;19:229–41.

Tumor-Suppressive Effects of Pannexin 1 in C6 Glioma Cells

Charles P.K. Lai, John F. Bechberger, Roger J. Thompson, et al.

Updated version	Access the most recent version of this article at: http://cancerres.aacrjournals.org/content/67/4/1545
Supplementary Material	Access the most recent supplemental material at: http://cancerres.aacrjournals.org/content/suppl/2007/02/09/67.4.1545.DC1

Cited articles	This article cites 42 articles, 16 of which you can access for free at: http://cancerres.aacrjournals.org/content/67/4/1545.full#ref-list-1
Citing articles	This article has been cited by 22 HighWire-hosted articles. Access the articles at: http://cancerres.aacrjournals.org/content/67/4/1545.full#related-urls

E-mail alerts	Sign up to receive free email-alerts related to this article or journal.
Reprints and Subscriptions	To order reprints of this article or to subscribe to the journal, contact the AACR Publications Department at pubs@aacr.org.
Permissions	To request permission to re-use all or part of this article, use this link http://cancerres.aacrjournals.org/content/67/4/1545. Click on "Request Permissions" which will take you to the Copyright Clearance Center's (CCC) Rightslink site.